JPET Fast Forward. Published on January 21, 2005 as DOI: 10.1124/jpet.104.080135

Mechanism of myricetin stimulation of vascular L-type Ca^{2+} current

Fabio Fusi, Giampietro Sgaragli, and Simona Saponara

Dipartimento di Scienze Biomediche, Università degli Studi di Siena, Siena, Italy

JPET Fast Forward. Published on January 21, 2005 as DOI: 10.1124/jpet.104.080135
This article has not been copyedited and formatted. The final version may differ from this version.

Running title

Myricetin stimulates vascular L-type Ca^{2+} current

Number of text pages: 27

Number of tables: 0

Number of figures: 8

Number of references: 39

Number of words in the Abstract: 246

Number of words in the Introduction: 448

Number of words in the Discussion: 1374

ABBREVIATIONS: Bay K 8644, (S)-(-)-methyl-1,4-dihydro-2,6-dimethyl-3-nitro-4-(2-trifluoromethylphenyl)pyridine-5-carboxylate; $I_{Ca(L)}$, L-type Ca^{2+} current; $I_{Ca(T)}$, T-type Ca^{2+} current; K_I, apparent dissociation constant for inactivated channels; K_R, apparent dissociation constant for resting channels; PSS, Physiological salt solution; V_h, holding potential.

Recommended section: Cardiovascular

JPET Fast Forward. Published on January 21, 2005 as DOI: 10.1124/jpet.104.080135
This article has not been copyedited and formatted. The final version may differ from this version.

ABSTRACT

An in-depth analysis of the mechanism of the L-type Ca^{2+} current [$I_{Ca(L)}$] stimulation induced by myricetin was performed in rat tail artery myocytes using the whole-cell patch-clamp method. Myricetin increased $I_{Ca(L)}$ in a frequency-, concentration- and voltage-dependent manner. At holding potentials (V_h) of –50 and –90 mV, the pEC_{50} values were 4.9±0.1 and 4.2±0.1, respectively; the latter corresponded to drug apparent dissociation constant for resting channels, K_R, of 67.6 μM. Myricetin shifted the maximum of the current-voltage relationship by 10 mV in the hyperpolarizing direction, but did not modify the threshold for $I_{Ca(L)}$ nor the T-type Ca^{2+} current. The Ca^{2+} channel blockers nifedipine, verapamil and diltiazem antagonized $I_{Ca(L)}$ in presence of myricetin. Myricetin increased the time to peak of $I_{Ca(L)}$ in a voltage- and concentration-dependent manner. Wash out reverted myricetin effect on both current kinetics and amplitude at V_h of –90 mV while reverting only current kinetics at V_h of –50 mV. At the latter V_h, myricetin shifted the voltage dependence of inactivation and activation curves to more negative potentials by 6.4 and 13.0 mV, respectively, in the mid-potential of the curves. At V_h of -90 mV, myricetin shifted, in a concentration-dependent manner, the voltage dependence of the inactivation curve to more negative potentials, with an apparent dissociation constant for inactivated channels (K_I) of 13.8 μM. Myricetin induced a frequency- as well as a V_h-dependent block of $I_{Ca(L)}$. In conclusion, myricetin behaves as an L-type Ca^{2+} channel agonist that stabilizes the channel in its inactivated state.

Food provides not only essential nutrients but also other bioactive compounds (e.g. flavonoids) good for health promotion and disease prevention (Middleton et al., 2000; WHO Technical Report Series 916). Regular consumption of fruit and vegetables, for example, is associated with reduced risk of cancer, cardiovascular disease, stroke, Alzheimer's disease, cataract, and some of the functional declines associated with aging (Liu 2003).

Red wine extracts, which are very rich in flavonoids, strongly inhibit, in bovine aortic endothelial cells, the synthesis of endothelin-1 (Corder et al., 2001), a vasoactive peptide that is linked to the development of coronary arteriosclerosis. Oral administration of red wine polyphenolic compounds has recently been shown to produce antihypertensive effects in both spontaneously hypertensive (Duarte et al., 2001) and deoxycorticosterone acetate-salt-hypertensive rats (Galisteo et al., 2004a; Galisteo et al., 2004b) as well as to decrease blood pressure in normotensive rats (Diebolt et al., 2001). In addition, red wine polyphenols increase nitric oxide production in rat aorta (Benito et al., 2002) *via* the intracellular Ca^{2+} increase in endothelial cells and activation of tyrosine kinases (Martin et al., 2002). These findings help to explain the French paradox (Renaud and de Lorgeril 1992) and the relationship between the Mediterranean diet based primarily on flavonoid-rich foods (Allium, Petroselinum and Brassica vegetables, and red wine) and the increased longevity (Orgogozo et al., 1997) accompanied by a low incidence of cardiovascular diseases in Mediterranean populations (Hertog et al., 1995).

The beneficial effect of flavonoids on human health, though highlighted in some prospective epidemiological studies, is not fully established (Hertog et al., 1997). Dietary flavonoids are found in human plasma in sub-µM or µM concentrations, either as aglycon or as glucosilate/glycosilate metabolites (Paganga and Rice-Evans 1997; Erlund et al., 2000; Scalbert and Williamson, 2000; Graefe et al., 2001) and some studies have clarified the molecular mechanisms of their effects on vascular tissues. Quercetin (3,3',4',5,7-

pentahydroxyflavone), although inducing both endothelium-dependent (Fusi et al., 2003b) and endothelium-independent vasorelaxation *in vitro* (Duarte et al., 1993; Herrera et al., 1996), has been demonstrated to be an effective stimulator of vascular smooth muscle L-type Ca^{2+} channels (Saponara et al., 2002). This effect, however, is paradoxically accompanied by vasorelaxation, which presumably takes place *via* pathways [e.g. PKC inhibition (see Duarte et al., 1993) *inter alias*], more prominent than L-type channel-mediated Ca^{2+} influx in the hierarchy of functional competences (Fusi et al., 2003b). Myricetin (3,3',4',5,5',7-hexahydroxyflavone) (Fig. 1a) was shown, recently, to increase $I_{Ca(L)}$ in rat tail artery myocytes and cause contraction in 20 mM KCl-depolarized rat aorta rings, without interacting with the dihydropyridine binding site (Fusi et al., 2003a).

The present study provides an in-depth analysis of the L-type Ca^{2+} channel stimulation performed by myricetin on isolated rat tail artery myocytes.

Materials and Methods

Cell isolation procedure. This study has been carried out in accordance with the Declaration of Helsinki and/or with the Guide for the Care and Use of Laboratory Animals as adopted and promulgated by the U.S. National Institutes of Health. Male Sprague-Dawley rats (350-450 g, Charles River Italia, Como, Italy) were anaesthetized with a mixture of Ketavet® (Gellini, Italy) and Rompum® (Bayer, Germany), decapitated and bled. Smooth muscle cells, freshly isolated from the tail main artery by means of collagenase treatment in the presence of BSA and trypsin inhibitor, as previously described (Fusi et al., 2001), exhibited an ellipsoid form (10-15 μm in width, 35-55 μm in length). The cells were continuously superfused with external solution containing 0.1 mM Ca^{2+} (PSS; see below for composition) using a peristaltic pump (LKB 2132), at a flow rate of 500 μl min^{-1}. At the end of each experiment, both the perfusion system and the bath were thoroughly rinsed once with ethanol and several times with water as well as, daily, with H_2O_2, to avoid contamination of any source. Electrophysiological responses were tested at room temperature (22-24°C) only in those cells that were phase dense. Cell membrane capacitance averaged 47.9±1.2 pF (*n*=71). The time constant of the voltage-clamp averaged 0.7±0.1 ms (*n*=71).

Whole-cell patch clamp recording. Conventional (Hamill et al., 1981) whole-cell patch-clamp method was employed to voltage-clamp smooth muscle cells. Recording electrodes were pulled from borosilicate glass capillaries (WPI, Berlin, Germany) and fire-polished to obtain a pipette resistance of 2-5 MΩ when filled with internal solution. A low-noise, high-performance Axopatch 200B (Axon Instruments, U.S.A.) patch-clamp amplifier driven by an IBM computer in conjunction with an A/D, D/A board (DigiData 1200 A/B series interface, Axon Instruments, U.S.A.) was used to generate and apply voltage pulses to the clamped

cells and record the corresponding membrane currents. Current signals, after compensation for whole-cell capacitance, series resistance and liquid junction potential, were low-pass filtered at 1 kHz and digitized at 3 kHz prior to being stored on the computer hard disk. I_{Ca} was always recorded in 5 mM Ca^{2+}-containing PSS: this concentration was shown to cause maximal peak current in arterial smooth muscle cells (Bolton et al., 1988).

I_{Ca} was measured over a range of test potentials of 250 ms duration from -50 mV to 70 mV from a holding potential (V_h) of -50 mV or –90 mV. Data were collected once the current amplitude had been stabilized (usually 7-10 min after the whole-cell configuration had been obtained). I_{Ca} did not run down during the following 30-40 minutes under these conditions.

To study the effect of some L-type Ca^{2+} channel antagonists (namely, nifedipine, diltiazem and verapamil) on $I_{Ca(L)}$ recorded in presence of myricetin, myocytes were pre-incubated with the flavonoid and, after a stable response had been attained, cumulative concentrations of the antagonists were added to the bath solution.

A two-pulses protocol was applied to record T-type Ca^{2+} currents [$I_{Ca(T)}$] avoiding overlap of $I_{Ca(L)}$. The cell was firstly depolarized for a 250-ms period to –40 mV from V_h of –90 mV to elicit $I_{Ca(T)}$. Following a 6 s return to the initial V_h, a 250-msec clamp pulse to 10 mV was applied to record $I_{Ca(L)}$, which was taken as 100%.

Steady-state inactivation curves, recorded twice from the same cell (in absence and presence of the drug, respectively), were obtained using a double-pulse protocol (Rubart et al., 1996). Once various levels of the conditioning potential had been applied for 5 s, followed by a short (5 ms) return to the V_h, a test pulse (250 ms) to 0 mV was delivered to evoke the current. Under control conditions, the 50% inactivation potential evaluated by fitting a Boltzmann distribution to the first curve was not significantly different from that of the second curve recorded after 10 min (see Fusi et al., 2002).

Activation curves were derived from the current-voltage relationships (see Fig. 2c). Conductance (G) was calculated from the equation $G=I_{Ca}/(E_m-E_{Ca})$, where I_{Ca} is the peak current elicited by depolarizing test pulses from –50 mV to 30 mV from V_h of –50 mV, E_m is the membrane potential, and E_{Ca} is the equilibrium potential for Ca^{2+} (181 mV, as estimated with the Nernst equation). G_{max} is the maximal Ca^{2+} conductance (calculated at potentials ≥ 10 mV). The ratio G/G_{max} was plotted against the membrane potential and fitted with the Boltzmann equation.

K^+ currents were blocked with 30 mM tetraethylammonium chloride in the PSS and Cs^+ in the internal solution (see below).

Current values were corrected for leakage using 300 µM Cd^{2+} which was assumed to block completely I_{Ca}.

Solutions and chemicals. PSS contained (in mM): 130 NaCl, 5.6 KCl, 10 HEPES, 20 glucose, 1.2 $MgCl_2$, 5 Na-pyruvate, 0.1 or 5 $CaCl_2$ (pH 7.4).

The internal solution for the conventional whole-cell method (pCa 8.4) consisted of (in mM): 105 CsCl, 10 HEPES, 11 EGTA, 2 $MgCl_2$, 1 $CaCl_2$, 5 Na-pyruvate, 5 succinic acid, 5 oxalacetic acid, 3 Na_2ATP and 5 phosphocreatine; pH was adjusted to 7.4 with CsOH.

The osmolarity of PSS (320 mosmol) and that of the internal solution (290 mosmol) (Stansfeld and Mathie 1993) were measured with an osmometer (Osmostat OM 6020, Menarini Diagnostics, Italy).

The chemicals used were: collagenase (type XI), tetraethylammonium chloride, BSA, trypsin inhibitor, nifedipine, diltiazem, verapamil, $CdCl_2$, and myricetin (Sigma-Aldrich, Italy). Myricetin dissolved directly in dimethylsulphoxide and nifedipine dissolved in ethanol, were diluted at least 1000 times in PSS, prior to use. The resulting concentrations of dimethylsulphoxide and ethanol (below 0.1%) failed to alter the current (data not shown).

Final drug concentrations are reported in the text. Unless otherwise stated, 20 μM myricetin was always used.

Following control measurements, each cell was exposed to a drug by flushing through the experimental chamber PSS containing that drug.

Statistical analysis. Acquisition and analysis of data were accomplished by using pClamp 8.2.0.232 software (Axon Instruments, U.S.A.) and GraphPad Prism version 3.03 (GraphPad Software, U.S.A.). Data are reported as mean±SEM; *n* is the number of cells analyzed (indicated in parentheses), isolated from at least 3 animals. Statistical analyses and significance as measured by either ANOVA (followed by Dunnett's post test) or Student's *t* test for unpaired and paired samples (two-tail) were obtained using GraphPad InStat version 3.05 (GraphPad Software, U.S.A.). In all comparisons, $p<0.05$ was considered significant. The current-voltage relationships were calculated on the basis of the peak values (leakage corrected) from the original currents. $I_{Ca(L)}$ activation was analyzed by measuring the time to peak current or the activation time constant (τ).

The pharmacological response to myricetin, described in terms of pEC_{50} (the negative logarithm to base 10 of the molar EC_{50}), was evaluated by global nonlinear regression (Motulsky and Christopoulolos, 2003), assuming that the drug did not affect the maximum of the concentration-response curve in cells clamped at V_h of –90 mV (Fig. 2a). The apparent dissociation constant for resting channels (K_R) was determined by holding the cells at –90 mV and measuring the corresponding concentration-response relationship for myricetin at 0.033 Hz. In fact, the number of channels in the resting state can be assayed by the $I_{Ca(L)}$ elicited by a large depolarization from hyperpolarized V_h (see Bean, 1984), such as -90 mV, where the entire population of L-type Ca^{2+} channels in rat tail artery myocytes is in the resting state (see Fig. 7), ready to open in response to depolarization.

JPET Fast Forward. Published on January 21, 2005 as DOI: 10.1124/jpet.104.080135
This article has not been copyedited and formatted. The final version may differ from this version.

Results

Effects of myricetin on $I_{Ca(L)}$ and $I_{Ca(T)}$. Fig. 2a (inset) shows a typical recording of $I_{Ca(L)}$ elicited with a clamp pulse to 0 mV from V_h of -90 mV under control conditions and after the addition of 100 μM myricetin. Myricetin enhanced $I_{Ca(L)}$ in a concentration-dependent manner (Fig. 2a) with an estimated pEC_{50} of 4.2±0.1 (*n*=3-6) that corresponded to a K_R of 67.6 μM. Myricetin enhanced $I_{Ca(L)}$ with a potency that depended upon V_h. In fact, when V_h was held at -50 mV, the concentration-dependent curve was shifted to the left (pEC_{50} of 4.9±0.1, *n*=3-6; *p*<0.001, Student's *t* test for unpaired samples).

Fig. 2b shows the time course of the effects of myricetin on the current recorded, at 0.033 Hz, from V_h of either -50 mV or –90 mV to a test potential of 0 mV. After $I_{Ca(L)}$ had reached steady values, the addition to bath solution of myricetin produced a gradual increase of the current that reached a plateau in about 3 min at all myricetin concentrations employed (data not shown). Noticeably, myricetin-induced stimulation of $I_{Ca(L)}$ was only partially reversible upon drug wash out at V_h of –50 mV, but completely reversible at V_h of –90 mV. At 2 Hz, under control conditions, the peak amplitude of $I_{Ca(L)}$ decreased rapidly to a steady-state value of about 70% of that recorded during the first pulse (data not shown). The addition of myricetin just after the first pulse of the second train of pulses, caused a similar decrease in peak amplitude of $I_{Ca(L)}$ followed by a partial recovery to a steady-state value of about 83% of that recorded during the first pulse (data not shown).

The current-voltage relationship in the conventional whole-cell configuration (Fig. 3) shows that myricetin significantly increased the peak inward current in the range between –30 mV and 10 mV, and shifted the apparent maximum by 10 mV in the hyperpolarizing direction without, however, varying the threshold at about –30 mV.

JPET Fast Forward. Published on January 21, 2005 as DOI: 10.1124/jpet.104.080135
This article has not been copyedited and formatted. The final version may differ from this version.

Myocytes here employed express both T- and L-type Ca^{2+} channels (see Petkov et al., 2001). I_{Ca} recorded at –40 mV from V_h of –90 mV was taken as an indicator of $I_{Ca(T)}$. This current, in fact, was no longer evident when V_h was –50 mV (data not shown). As shown in Fig. 4b and c, myricetin still increased $I_{Ca(L)}$ at 10 mV, although with a lower efficacy as compared to V_h of –50 mV (see Fig. 3c). On the contrary, $I_{Ca(T)}$ was not significantly modified by myricetin (Fig. 4a and c) even at a concentration of 100 μM (data not shown).

Inhibition by some L-type Ca^{2+} channel blockers of $I_{Ca(L)}$ recorded in the presence of myricetin. The antagonistic effects of nifedipine, diltiazem and verapamil were determined after a stable response to myricetin, at V_h of –50 mV, was attained. All three Ca^{2+} channel blockers antagonized, in a concentration-dependent manner, and fully blocked $I_{Ca(L)}$ recorded in presence of myricetin (Fig. 5), showing pIC_{50} values of 8.0±0.2 (nifedipine, *n*=5), 5.7±0.1 (diltiazem, *n*=5), and 6.0±0.1 (verapamil, *n*=5), respectively.

Effects of myricetin on $I_{Ca(L)}$ kinetics. The current evoked at 0 mV from V_h of either -50 mV or –90 mV activated and then declined with a time course that could be fitted by a mono-exponential equation, with a τ of activation of 3.0±0.3 ms and 2.02±0.1 ms, and a τ of inactivation of 109.9±9.5 ms (*n*=5) and 85.9±4.2 ms (*n*=6), respectively. In the presence of myricetin, activation was delayed and its time course could be fitted by a bi-exponential equation at V_h of –50 mV (τ_1=3.4±0.6 ms and τ_2=18.9±2.9 ms) and by a mono-exponential equation at V_h of –90 mV (τ=3.6±0.5 ms; $p<0.01$, Student's *t* test for paired samples), respectively. This delay in activation, however, markedly reduced the length of the inactivating segment of traces at V_h of –50 mV thus impeding its fitting; that at V_h of –90 mV increased to 199.3±10.7 ms ($p<0.01$). The effect of myricetin on the current kinetics was reversible upon wash out and both τ of activation and τ of inactivation returned to control

JPET Fast Forward. Published on January 21, 2005 as DOI: 10.1124/jpet.104.080135
This article has not been copyedited and formatted. The final version may differ from this version.

values (3.0±0.4 ms and 114.2±14.6 ms, at V_h of –50 mV, and 2.6±0.2 ms and 96.4±10.3 ms, at V_h of –90 mV, respectively).

Myricetin prolonged the time to peak of $I_{Ca(L)}$ in a voltage- (Fig. 5a) and concentration-dependent manner (Fig. 5b), the latter showing a bell-shaped pattern.

Effects of myricetin on steady-state inactivation and activation curves for $I_{Ca(L)}$. The voltage dependence of myricetin stimulation was assessed by determining the steady-state inactivation and activation curves for $I_{Ca(L)}$. At V_h of -50 mV, myricetin significantly shifted the steady-state inactivation curve to more negative potentials (Fig. 7a). The 50% inactivation potentials, evaluated by means of the Boltzmann fitting procedure, were -24.2±1.9 mV (control) and -30.7±1.5 mV (myricetin; n=5; p<0.01, Student's t test for paired samples), respectively. Furthermore, the slope was significantly steeper in the presence of myricetin (slope factor=-8.1±0.7 mV, control, and -6.4±0.7 mV, myricetin; p<0.05).

The activation curves calculated from the current-voltage relationships in Fig. 3c were fitted with the Boltzmann equation (Fig. 7a). Myricetin reduced both the 50% activation potential from –2.5±0.7 mV to –13.6±0.6 mV (n=5; p<0.001, Student's t test for paired samples) and the slope factor from 6.6±0.1 mV to 6.1±0.2 mV (P>0.05).

The apparent dissociation constant of myricetin for inactivated channels (K_I) was determined by the shift of Ca^{2+} channel steady-state availability as a function of myricetin concentration at V_h of -90 mV (Bean et al., 1983). Myricetin shifted the 50% inactivation potential to more hyperpolarizing values in a concentration-dependent manner (Fig. 7b); however, it did not modify the slope factors (-6.7±0.3 mV, control, n=11; -6.3±0.6 mV, 3 μM myricetin, n=3; -5.9±0.4 mV, 10 μM myricetin, n=3; -6.7±0.1 mV, 20 μM myricetin, n=3; -6.4±0.2 mV, 100 μM myricetin, n=4). K_I was estimated by plotting the 50% inactivation potentials as a function of myricetin concentration. This relationship fitted the equation

$$V_{50}=K_{control} \times \ln\{1/[1+([drug]/K_I)]\}+V_{50\ control}$$

JPET Fast Forward. Published on January 21, 2005 as DOI: 10.1124/jpet.104.080135
This article has not been copyedited and formatted. The final version may differ from this version.

where $V_{50\ control}$ and $K_{control}$ were the values of the 50% inactivation potential and the slope measured in control conditions, respectively. The value of K_I thus determined was 13.8±2.7 μM.

Frequency-dependent block of $I_{Ca(L)}$ by myricetin. The frequency-dependence of myricetin-induced effects on $I_{Ca(L)}$ was assessed, as shown in Fig. 8. In the absence of myricetin, twenty depolarizing pulses of 50-ms duration to 0 mV from V_h of -50 mV were applied at different pulse intervals, ranging from 0.5 to 2 s (namely 2, 1, and 0.5 Hz) (Fig. 8a). At the end of the protocol, myricetin was added to the bath solution and, after a 4-min interval without stimulation, the same protocol was repeated. In control conditions, the peak amplitude of $I_{Ca(L)}$ evoked by the 20th pulse decreased significantly as the frequency of stimulation increased (Fig. 8b, inset), thus suggesting a cumulative channel inactivation. Externally applied myricetin produced a frequency-dependent block of $I_{Ca(L)}$, the highest frequency causing the greatest inhibition. The frequency-dependent block, calculated by normalizing the current amplitude evoked by the 20th applied stimulus against that induced by the first step-pulse, was significantly lower than that observed under the corresponding control conditions only at 2 Hz (Fig. 8b, inset). Similar results were obtained in parallel experiments wherein Ba^{2+} was substituted for Ca^{2+} as charge carrier (data not shown).

The frequency-dependent block of $I_{Ca(L)}$ by myricetin depended upon V_h (Fig. 8b). In fact, the residual current recorded at the 20th applied stimulus (2 Hz) from V_h of -50 mV was 57.9±3.4% (n=3), whereas that from V_h of -90 mV was 91.8±1.2% (n=3, p<0.001, Student's t test for unpaired samples) (Fig. 8b, inset).

JPET Fast Forward. Published on January 21, 2005 as DOI: 10.1124/jpet.104.080135
This article has not been copyedited and formatted. The final version may differ from this version.

Discussion

The present study provides an in-depth analysis of myricetin-induced stimulation of vascular smooth muscle L-type Ca^{2+} channels. This flavonoid acted on L-type, but not T-type Ca^{2+} channels, in a voltage-, concentration- as well as frequency-dependent manner. A characteristic of myricetin-induced enhancement of $I_{Ca(L)}$ was a marked tonic effect, which developed independently of channel activation. In fact, at 0.033 Hz, a frequency allowing full recovery of rat tail artery myocytes Ca^{2+} channels from inactivation (see Saponara et al., 2002), the amplitude of $I_{Ca(L)}$ was increased by myricetin, in a way that was also dependent on V_h. Furthermore, the amplitude of the first $I_{Ca(L)}$, recorded after a 4-min silent interval subsequent to myricetin addition, increased to a value identical to that obtained gradually in cells stimulated at a frequency of 0.033 Hz for 4 min in the presence of myricetin. This suggests that myricetin does not need an open channel to have access to its putative binding site and display its stimulatory activity (tonic stimulation).

Myricetin induced a peak current enhancement which reached maximum values at weak depolarization conditions becoming progressively smaller by increasing membrane depolarization, and shifted the maximum of the current-voltage relationship towards more negative potentials without affecting the threshold for $I_{Ca(L)}$. Thus, the effect of myricetin on the current-voltage relationship might be explained, at least in part, by the activation curve shift towards more hyperpolarizing potentials, which was more pronounced than that observed in the inactivation curve. In addition, myricetin caused a significant change in the slope of the inactivation curve. These results indicate that myricetin may alter the voltage sensitivity of the channel inactivation mechanism. Furthermore, myricetin strongly slowed Ca^{2+} channel activation kinetics in a concentration-dependent manner as well as over a wide range of membrane potentials, although this effect was more pronounced at weak

depolarization values. The fact that myricetin slowed the time-course of current activation while also shifting the steady-state activation curve to more negative potentials, can be explained assuming that the flavonoid, besides affecting the voltage-dependency of the channels, also interferes with Ca^{2+}-channel gating kinetics, slowing (i.e. increasing the rate constants of) the transition from the closed to the open state of the channel. In other ways it modifies the gating mechanisms. These observations demonstrate that the two effects depend on myricetin occupancy of binding sites at least partly distinct. A similar phenomenon has been recently described for a series of divalent cations (Castelli et al., 2003). Finally, the inward tail currents decayed more slowly in the presence of myricetin (data not shown), possibly as a consequence of the longer-lasting opening of the channel.

Taken together, all these elements indicate that myricetin shares several basic features with some Ca^{2+} channel agonists such as (S)-(-)-methyl-1,4-dihydro-2,6-dimethyl-3-nitro-4-(2-trifluoromethylphenyl)pyridine-5-carboxylate (Bay K 8644; Wang et al., 1989; Fusi et al., 2003a) and the structural related flavonoid quercetin (see below; Saponara et al., 2002).

Another feature of myricetin action is the frequency-dependent block of $I_{Ca(L)}$. Frequency-dependent block of $I_{Ca(L)}$ and shift of the channel availability towards more hyperpolarizing potentials are generally observed with drugs possessing a greater affinity for the channel in its inactivated state. In fact, myricetin, like verapamil (McDonald et al., 1994), inhibited $I_{Ca(L)}$ in a frequency-dependent fashion (use-dependent block), i.e. the repetitive depolarization at a relatively high frequency of stimulation potentiated the inhibition of $I_{Ca(L)}$. Noticeably, this phenomenon was observed also in the presence of Ba^{2+} as charge carrier. Therefore, a direct drug effect, rather than a Ca^{2+}-dependent inactivation of the channel subsequent to current stimulation, seems to be implicated. Furthermore, myricetin, like nicardipine (Bean 1984), shifted the voltage dependence of the inactivation curve to more negative potentials. Taken together, these observations indicate that myricetin stabilizes L-type Ca^{2+} channels in their

JPET Fast Forward. Published on January 21, 2005 as DOI: 10.1124/jpet.104.080135
This article has not been copyedited and formatted. The final version may differ from this version.

inactivated state (see Bean, 1984) in a voltage-dependent manner. Moreover, its apparent dissociation constant for the inactivated channel (K_I) was about 5 times lower than that for the closed channel (K_R), thus providing an explanation for the shift of the concentration-response curve for $I_{Ca(L)}$ stimulation, recorded at two different V_h, towards higher drug concentrations. In fact, there was a significant shift of the curve to the right at V_h of –90 mV, i.e. at a greater membrane hyperpolarization, where a smaller number of channels are supposed to be in the inactivated state. Interestingly, also the effects of myricetin on both $I_{Ca(L)}$ kinetics (activation and inactivation) and the slope of steady-state inactivation curve were affected by V_h, being less pronounced when cell membrane potential was held at -90 mV as compared to -50 mV. The reduced drug sensitivity at V_h of -90 mV further supports the hypothesis of a higher affinity of myricetin for the channel in the inactivated state.

Several studies demonstrate how, under certain conditions, drugs affecting L-type Ca^{2+} channels (e.g. dihydropyridines, phenylalkylamines, and benzothiazepines) can have opposite effects on $I_{Ca(L)}$, i.e. inhibition if activators and activation if blockers (McDonald et al., 1994). Some conditions promote the block of L-type Ca^{2+} channels by dihydropyridine agonists such as Bay K 8644; in particular, high drug concentrations, depolarized V_h, and high pulsing rates. Though the first of these conditions could not be evaluated in the present study owing to solubility limits of myricetin, the latter two well applied to the flavonoid. In fact, pulsing rates higher than 1 Hz converted the agonist myricetin into a blocking agent while depolarized V_h favored the progressive accumulation of this block when the interstimulus interval was short. Under these experimental conditions, the blocking activity of the L-type Ca^{2+} channel agonist myricetin clearly emerged.

It might be argued that myricetin effects on $I_{Ca(L)}$ are not due only to its action on L-type Ca^{2+} channels but rather the consequence of the recruitment of a third type of Ca^{2+} channel, i.e. N-type Ca^{2+} channel. However, the observed, complete block of the current induced by

JPET Fast Forward. Published on January 21, 2005 as DOI: 10.1124/jpet.104.080135
This article has not been copyedited and formatted. The final version may differ from this version.

the three well known L-type Ca^{2+} channel blockers nifedipine, diltiazem, and verapamil, in cells exposed to myricetin, did not substantiate this hypothesis.

Previous studies have shown how quercetin stimulates $I_{Ca(L)}$ in cells isolated from rat tail artery (Saponara et al., 2002), in clonal rat pituitary GH_4C_1 (Summanen et al., 2001) as well as GH_3 cells, but not in neuronal NG108-15 cells (Wu et al., 2003). The electrophysiological characteristics of myricetin Ca^{2+} channel agonism described here (degree of current enhancement, time for maximal effect development, stimulation of current-voltage relationship, stabilization of the inactivated state, lack of effects on $I_{Ca(T)}$, modulation of voltage-dependency and kinetics of the current) are similar to those already observed with quercetin in the same experimental model (Saponara et al., 2002). Myricetin stimulation of $I_{Ca(L)}$, however, only partially reverted upon wash out of the drug at V_h of –50 mV, at variance with the effect on current kinetics; moreover, myricetin enhancement of $I_{Ca(L)}$ at V_h of –90 mV, as well as that of $I_{Ba(L)}$ in the same preparation (Fusi et al., 2003a), were fully reversible. It can be hypothesized that Ca^{2+} ion occupies a high-affinity Ca^{2+} binding site, thus stabilizing the putative myricetin-binding site, as it is the case with dihydropyridine Ca^{2+} antagonists (Mitterdorfer et al., 1998). This would take place in the inactivated state of the channel, where a single Ca^{2+} ion is tightly coordinated at the selectivity filter, and the putative myricetin binding domain would assume a high-affinity binding conformation for the drug, thus allowing the formation of a ternary complex. This complex is assumed to stabilize the channel in its inactivated state. Therefore, the replacement of Ca^{2+} with Ba^{2+} as a charge carrier, as well as the decrease in proportion of inactivated channels at more hyperpolarized V_h, should turn the putative myricetin binding domain into a low affinity binding conformation, thus allowing the complete wash out of the drug and the ensuing full reversion of its effects. Of course, this model does not apply to the effects of myricetin on current kinetics that turned to control values even in the presence of Ca^{2+} at V_h of –50 mV,

once more supporting the hypothesis that the flavonoid interacts with distinct sites of the channel protein.

In conclusion, the present electrophysiological data point to myricetin as a vascular L-type Ca^{2+} channel agonist characterized by a greater affinity for the channel in the inactivated state. Thus, quercetin and myricetin appear as members of a new class of L-type Ca^{2+} channel modulators of natural source.

References

Bean BP (1984) Nitrendipine block of cardiac calcium channels: high-affinity binding to the inactivated state. *Proc Natl Acad Sci USA* **81**:6388-6392.

Bean BP, Cohen CJ and Tsien RW (1983) Lidocaine block of cardiac sodium channels. *J Gen Physiol* **81**:613-642.

Benito S, Lopez D, Sáiz MP, Buxaderas S, Sánchez J, Puig-Parellada P and Mitjavila MT (2002) A flavonoid-rich diet increases nitric oxide production in rat aorta. *Br J Pharmacol* **35**:910-916.

Bolton TB, Aaronson PI and MacKenzie I (1988) Voltage-dependent calcium channel in intestinal and vascular smooth muscle cells. *Ann N Y Acad Sci* **522**:32-42.

Castelli L, Tanzi F, Taglietti V and Magistretti J (2003). Cu^{2+}, Co^{2+} and Mn^{2+} modify the gating kinetics of high-voltage-activated Ca^{2+} channels in rat palaeocortical neurons. *J Membr Biol* **195**:121-136.

Corder R, Douthwaite JA, Lees DM, Khan NQ, Viseu Dos Santos AC, Wood EG and Carrier MJ (2001) Endothelin-1 synthesis reduced by red wine. *Nature* **414**:863-864.

Diebolt M, Bucher B and Andriantsitohaina R (2001) Wine polyphenols decrease blood pressure, improve NO vasodilatation, and induce gene expression. *Hypertension* **38**:159-165.

Duarte J, Perez-Vizcaino F, Zarzuelo A, Jimenez J and Tamargo J (1993) Vasodilator effects of quercetin in isolated rat vascular smooth muscle. *Eur J Pharmacol* **239**:1-7.

Duarte J, Perez-Palencia R, Vargas F, Ocete MA, Perez-Vizcaino F, Zarzuelo A and Tamargo J (2001) Antihypertensive effects of the flavonoid quercetin in spontaneously hypertensive rats. *Br J Pharmacol* **133**:117-124.

Erlund I, Kosonen T, Alfthan G, Maenpaa J, Perttunen K, Kenraali J, Parantainen J and Aro A (2000) Pharmacokinetics of quercetin from quercetin aglycone and rutin in healthy volunteers. *Eur J Clin Pharmacol* **56**:545-553.

Fusi F, Saponara S, Gagov H and Sgaragli GP (2001) 2,5-Di-*t*-butyl-1,4-benzohydroquinone (BHQ) inhibits vascular L-type Ca^{2+} channel via superoxide anion generation. *Br J Pharmacol* **133**:988-996.

Fusi F, Saponara S, Sgaragli G, Cargnelli G and Bova S (2002) Ca^{2+} entry blocking and contractility promoting actions of norbormide in single rat caudal artery myocytes. *Br J Pharmacol* **137**:323-328.

Fusi F, Saponara S, Frosini M, Gorelli B and Sgaragli G (2003a) L-type Ca^{2+} channels activation and contraction elicited by myricetin on vascular smooth muscles. *Naunyn Schmiedeberg's Arch Pharmacol* **368**:470-478.

Fusi F, Saponara S, Pessina F, Gorelli B and Sgaragli G (2003b) Effects of quercetin and rutin on vascular preparations. A comparison between mechanical and electrophysiological phenomena. *Eur J Nutr* **42**:10-17.

Galisteo M, Garcia-Saura MF, Jimenez R, Villar IC, Wangensteen R, Zarzuelo A, Vargas F and Duarte J (2004a) Effects of quercetin treatment on vascular function in deoxycorticosterone acetate-salt hypertensive rats. Comparative study with verapamil. *Planta Med* **70**:334-341.

Galisteo M, Garcia-Saura MF, Jimenez R, Villar IC, Zarzuelo A, Vargas F and Duarte J (2004b) Effects of chronic quercetin treatment on antioxidant defence system and oxidative status of deoxycorticosterone acetate-salt-hypertensive rats. *Mol Cell Biochem* **259**:91-99.

Graefe EU, Wittig J, Mueller S, Riethling AK, Uehleke B, Drewelow B, Pforte H, Jacobasch G, Derendorf H and Veit M (2001) Pharmacokinetics and bioavailability of quercetin glycosides in humans. *J Clin Pharmacol* **41**:492-499.

Hamill OP, Marty A, Neher E, Sakmann B and Sigworth FJ (1981) Improved patch-clamp techniques for high-resolution current recording from cells and cell-free membrane patches. *Pflügers Arch* **391**:85-100.

Herrera MD, Zarzuelo A, Jimenez J, Marhuenda E and Duarte J (1996) Effects of flavonoids on rat aortic smooth muscle contractility: structure-activity relationships. *Gen Pharmacol* **27**:273-277.

Hertog MG, Kromhout D, Aravanis C, Blackburn H, Buzina R, Fidanza F, Giampaoli S, Jansen A, Menotti A, Nedeljkovic S, Pekkarinen M, Simic BS, Toshima H, Feskens EJM, Hollman PCH and Katan MB (1995) Flavonoid intake and long-term risk of coronary heart disease and cancer in the seven countries study. *Arch Intern Med* **155**:381-386.

Hertog MG, Feskens EJ and Kromhout D (1997) Antioxidant flavonols and coronary heart disease risk. *Lancet* **349**:699.

Liu RH (2003) Health benefits of fruit and vegetables are from additive and synergistic combinations of phytochemicals. *Am J Clin Nutr* **78**:517S-520S.

Martin S, Andriambeloson E, Takeda K and Andriantsitohaina R (2002) Red wine polyphenols increase calcium in bovine aortic endothelial cells: a basis to elucidate signalling pathways leading to nitric oxide production. *Br J Pharmacol* **35**:1579-1587.

McDonald TF, Pelzer S, Trautwein W and Pelzer DJ (1994) Regulation and modulation of calcium channels in cardiac, skeletal, and smooth muscle cells. *Physiol Rev* **74**:365-507.

Middleton EJr, Kandaswami C and Theoharides TC (2000) The effects of plant flavonoids on mammalian cells: implications for inflammation, heart disease, and cancer. *Pharmacol Rev* **52**:673-751.

Mitterdorfer J, Grabner M, Kraus RL, Hering S, Prinz H, Glossmann H and Striessnig J (1998) Molecular basis of drug interaction with L-type Ca^{2+} channels. *J Bioenerg Biomembr* **30**:319-334.

Motulsky HJ and Christopoulolos A (2003). *Fitting models to biological data using nonlinear regression. A practical guide to curve fitting*. GraphPad Software Inc., San Diego.

Orgogozo JM, Dartigues JF, Lafont S, Letenneur L, Commenges D, Salamon R, Renaud S and Breteler MB (1997) Wine consumption and dementia in the elderly: a prospective community study in the Bordeaux area. *Rev Neurol* **153**:185-192.

Paganga G and Rice-Evans CA (1997) The identification of flavonoids as glycosides in human plasma. *FEBS Lett* **401**:78-82.

Petkov GV, Fusi F, Saponara S, Gagov H, Sgaragli GP and Boev KK (2001) Characterization of voltage-gated calcium currents in freshly isolated smooth muscle cells from rat tail main artery. *Acta Physiol Scand* **173**:257-265.

Renaud S and de Lorgeril M (1992) Wine, alcohol, platelets, and the French paradox for coronary heart disease. *Lancet* **339**:1523-1526.

Rubart M, Patlak JB and Nelson MT (1996) Ca^{2+} currents in cerebral artery smooth muscle cells of rat at physiological Ca^{2+} concentrations. *J Gen Physiol* **107**:459-472.

Saponara S, Sgaragli G and Fusi F (2002) Quercetin as a novel activator of L-type Ca^{2+} channels in rat tail artery smooth muscle cells. *Br J Pharmacol* **135**:1819-1827.

Scalbert A and Williamson G (2000). Dietary intake and bioavailability of polyphenols. *J Nutr* **130**:2073S-85S.

Stansfeld C and Mathie A (1993) Recording membrane currents of peripheral neurones in short-term culture, in: *Electrophysiology. A practical approach* (Wallis DI eds) pp 3-28, IRL Press, Oxford.

Summanen J, Vuorela P, Rauha JP, Tammela P, Marjamaki K, Pasternack M, Tornquist K and Vuorela H (2001) Effects of simple aromatic compounds and flavonoids on Ca^{2+} fluxes in rat pituitary GH_4C_1 cells. *Eur J Pharmacol* **414**:125-133.

Wang R, Karpinski E and Pang PK (1989) Two types of calcium channels in isolated smooth muscle cells from rat tail artery. *Am J Physiol* **256**:H1361-H1368.

WHO Technical Report Series 916. Diet, nutrition and the prevention of chronic diseases. diseases: report of a joint WHO/FAO expert consultation, Geneva, 28 January - 1 February 2002.

Wu SN, Chiang HT, Shen AY and Lo YK (2003) Differential effects of quercetin, a natural polyphenolic flavonoid, on L-type calcium current in pituitary tumor (GH3) cells and neuronal NG108-15 cells. *J Cell Physiol* **195**:298-308.

Footnotes

This work was supported by grants from the Università degli Studi di Siena [PAR 2002 and 2001 Young Researcher (to S.S.)], and a grant from the Tuscany Region (Carabiotech 2002).

Address correspondence to: Dr. Fabio Fusi, Dipartimento di Scienze Biomediche, Università degli Studi di Siena, via A. Moro 2, 53100 Siena, Italy. Tel.: +39-0577-234438. Fax: +39-0577-234446. E-mail: fusif@unisi.it

JPET Fast Forward. Published on January 21, 2005 as DOI: 10.1124/jpet.104.080135
This article has not been copyedited and formatted. The final version may differ from this version.

Legends for figures

Fig. 1. Molecular structure of myricetin (3,3',4',5,5',7-hexahydroxyflavone).

Fig. 2. Myricetin stimulation of $I_{Ca(L)}$ in rat tail artery myocytes. (a) Concentration-effect relationship at various V_h. On the ordinate scale, response is reported as percent of control. The curves show the best fit of the points (pEC_{50}=4.9±0.1, n_H=1.1, at V_h of –50 mV, and 4.2±0.1, n_H=1.1, at V_h of –90 mV, respectively). Data points are means±SEM (*n*=3-6). Inset: original recordings of conventional whole-cell $I_{Ca(L)}$ elicited with 250-ms clamp pulses to 0 mV from V_h of -90 mV (see schematic diagram), measured in absence (control) or presence of myricetin (100 μM). (b) Time course of $I_{Ca(L)}$ stimulation induced by myricetin at various V_h. Myricetin (20 μM) was applied, at the time indicated by the arrow, and peak currents were recorded during a typical depolarization from either –50 mV or –90 mV to 0 mV, applied every 30 s (0.033 Hz), and subsequently normalized according to the current recorded just prior to myricetin application. Drug wash out gives rise either to partial recovery at V_h of –50 mV, or to full recovery, at V_h of –90 mV, from the stimulation. $I_{Ca(L)}$ suppression by 300 μM Cd^{2+} is also shown. Data points are mean±SEM (*n*=6).

Fig. 3. Effect of myricetin on $I_{Ca(L)}$-voltage relationship in rat tail artery myocytes. (a, b) Original recordings of conventional whole-cell $I_{Ca(L)}$ elicited with 250-ms clamp pulses from V_h of -50 mV to test potentials in the range –50 mV to 70 mV (see schematic diagram), measured in absence (control) or presence of myricetin (20 μM). (c) Current-voltage relationships constructed prior to the addition of myricetin (control) and in the presence of myricetin. Data points are mean±SEM (*n*=5). * $p<0.05$, ** $p<0.01$, Student's *t* test for paired samples.

Fig. 4. Effect of myricetin on $I_{Ca(T)}$ in rat tail artery myocytes. (a, b) Original recordings of conventional whole-cell I_{Ca} elicited with 250-ms clamp pulses to -40 mV (a) and 10 mV (b) from V_h of -90 mV (6-s interpulse; see schematic diagram) measured in absence (control) or presence of myricetin (20 μM). The two traces in panel (a) are superimposed. (c) The currents measured during the depolarizing pulse to both –40 mV and 10 mV from V_h of –90 mV were expressed as a percentage of the current evoked by a clamp pulse to 10 mV under control conditions. Each column with the relative bar represents the mean±SEM (*n*=4).

Fig. 5. Effects of nifedipine, diltiazem, and verapamil on $I_{Ca(L)}$ amplitude recorded in presence of myricetin in rat tail artery myocytes. The amplitude of the current recorded during a typical depolarization from -50 mV to 0 mV in the presence of myricetin was normalized as 100%. Data points are mean±SEM (*n*=5).

Fig. 6. Effects of myricetin on time to peak for $I_{Ca(L)}$ activation in rat tail artery myocytes. (a) Time to peak for activation, measured at various membrane potentials, in absence (control) or presence of myricetin. Columns are mean±SEM (*n*=5). * $p<0.05$, ** $p<0.01$, *** $p<0.001$, Student's *t* test for paired samples. (b) Time to peak for activation, measured in absence (control) or presence of different concentrations of myricetin (0.1-100 μM). Columns and relative bars represent mean±SEM (*n*=3-7). ** $p<0.01$, Dunnett's post test. Inset: original recordings of conventional whole-cell $I_{Ca(L)}$ elicited with 250-ms clamp pulses to 0 mV from V_h of -50 mV, measured in absence (control) or presence of myricetin.

Fig. 7. Effect of myricetin on both $I_{Ca(L)}$ activation and inactivation curves in rat tail artery myocytes. (a) Steady-state inactivation curves recorded from V_h of –50 mV, obtained in

absence (control) and presence of myricetin, were fitted to the Boltzmann equation. Peak current values were used. Steady-state inactivation curves were obtained using the double-pulse protocol (see Methods section). The current measured during the test pulse is plotted against membrane potential and expressed as relative amplitude. Activation curves were obtained from the current-voltage relationships of Fig. 2c and fitted to the Boltzmann equation (see Methods section). Data point represents the mean±SEM (n=5). (b) Effect of various concentrations of myricetin (3-100 μM) on 50% inactivation potentials obtained from steady-state inactivation curves recorded from V_h of -90 mV, in absence (control) and presence of myricetin, and fitted to the Boltzmann equation. Columns are mean±SEM (n=3-11). ** $p<0.01$, Dunnett's post test.

Fig. 8. Tonic stimulation and frequency-dependent block of $I_{Ca(L)}$ by myricetin in rat tail artery myocytes. Tonic and frequency dependence of myricetin-induced effects were examined in the range 0.5-2 Hz. In absence of myricetin, twenty depolarizing 50-ms clamp pulses to 0 mV from V_h of either -50 mV (a) or -90 mV (b) were applied at 0.5, 1, or 2 Hz, respectively. Myricetin was added just after the delivery of the first train of pulses and after a 4 min pause the same protocol was repeated. The peak amplitude elicited by the first pulse at each frequency in the absence of myricetin was taken as 100%. Inset: the peak amplitude elicited by the first pulse of each train (either in absence or in presence of myricetin) was taken as 100%, to better appreciate frequency-dependent block of $I_{Ca(L)}$. Data points are mean±SEM (n=3). * $p<0.05$ vs. the 20th pulse recorded in control condition at 2 Hz, † $p<0.05$ vs. the 20th pulse recorded in control condition at 0.5 Hz, ‡ $p<0.001$ vs. the 20th pulse recorded in presence of myricetin at 2 Hz, Student's t test for paired samples or Bonferroni post test, respectively.

Fig. 1

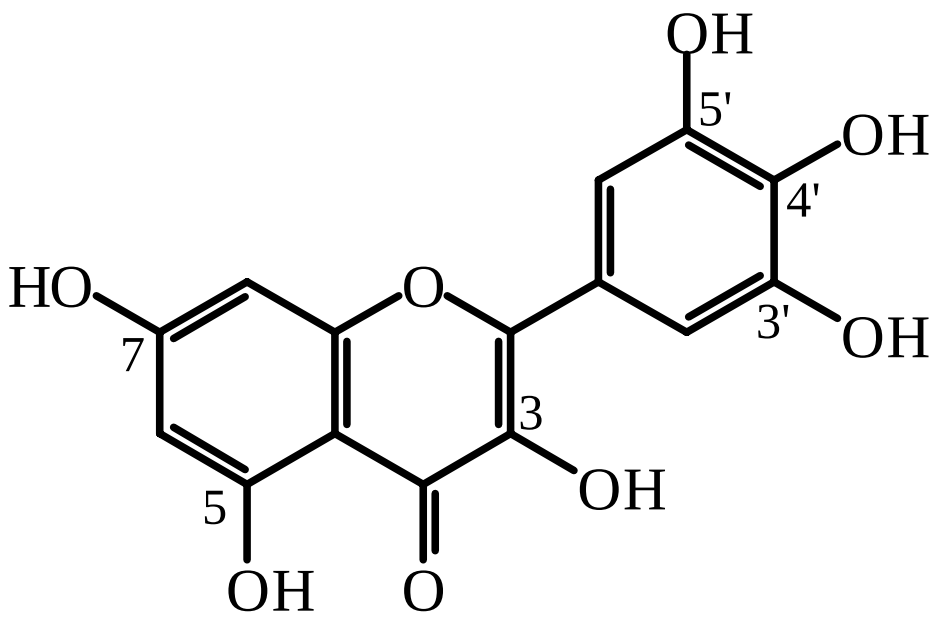

JPET Fast Forward. Published on January 21, 2005 as DOI: 10.1124/jpet.104.080135
This article has not been copyedited and formatted. The final version may differ from this version.

Fig. 2

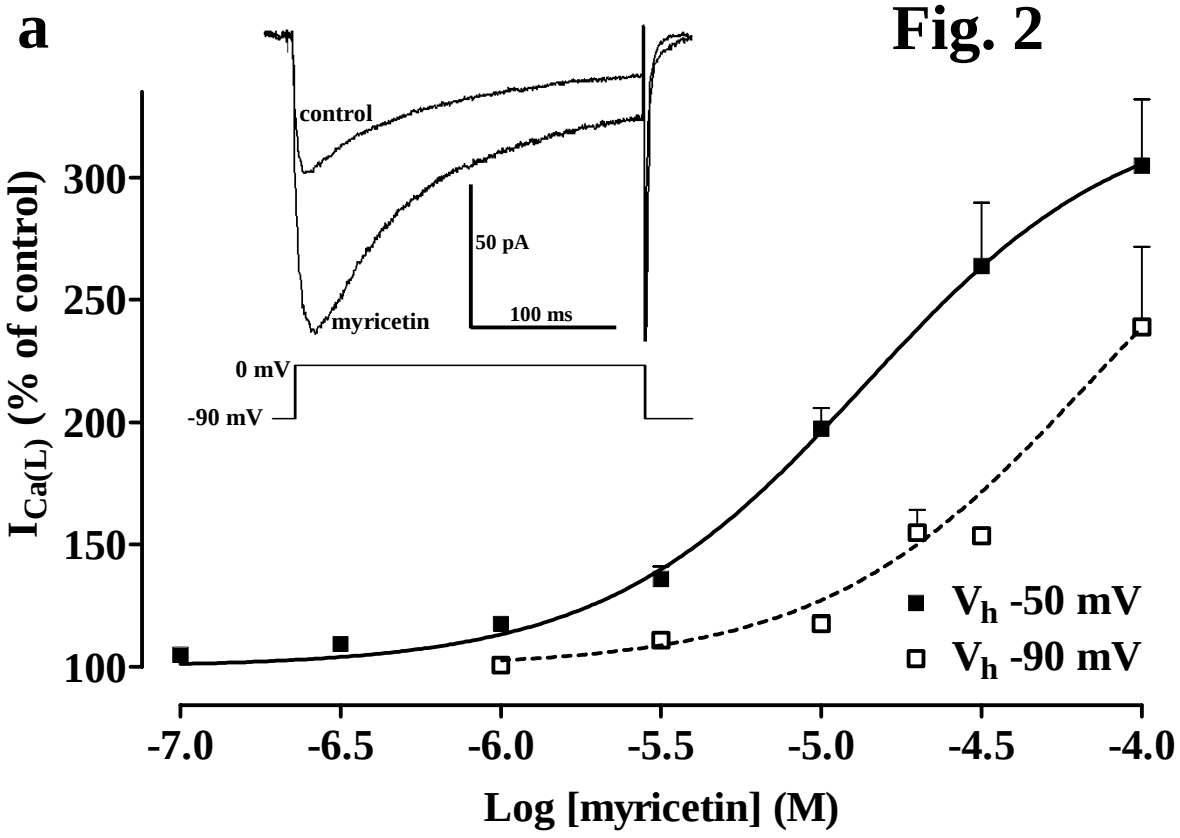

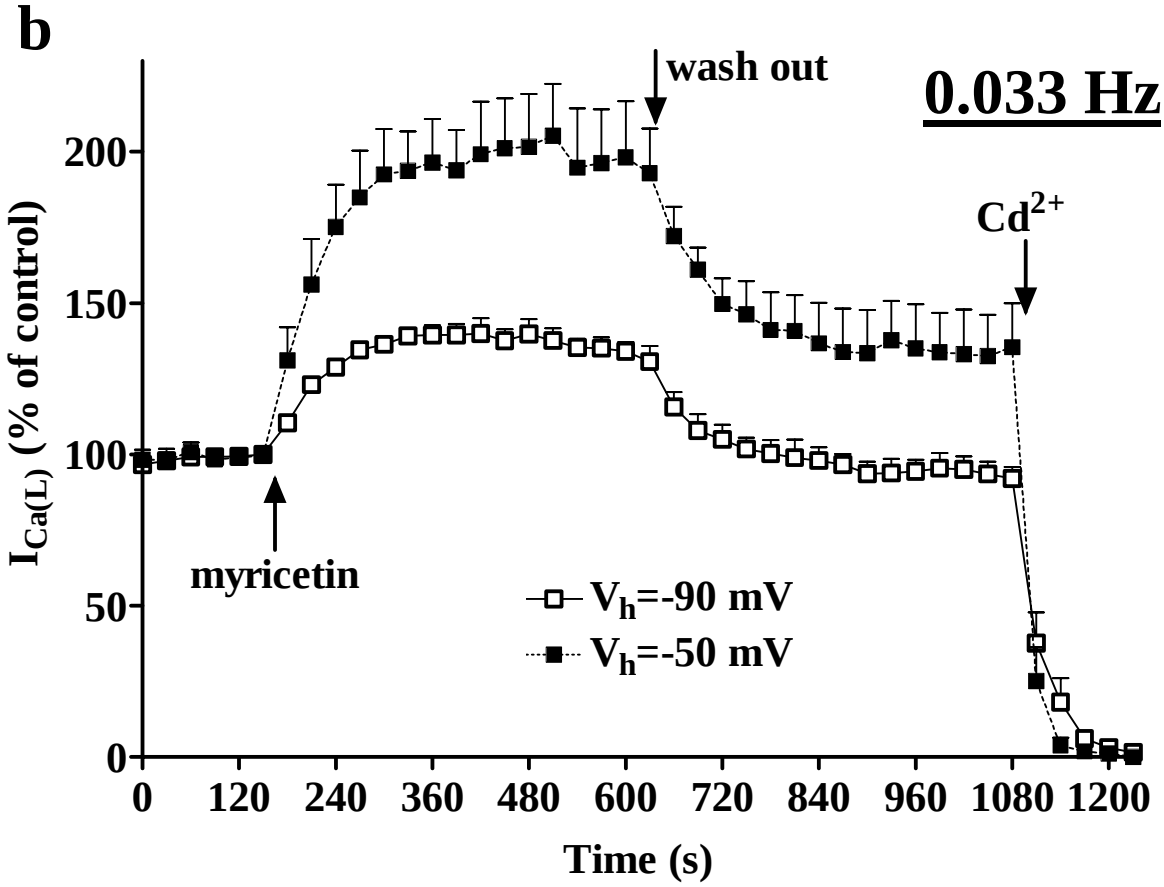

Fig. 3

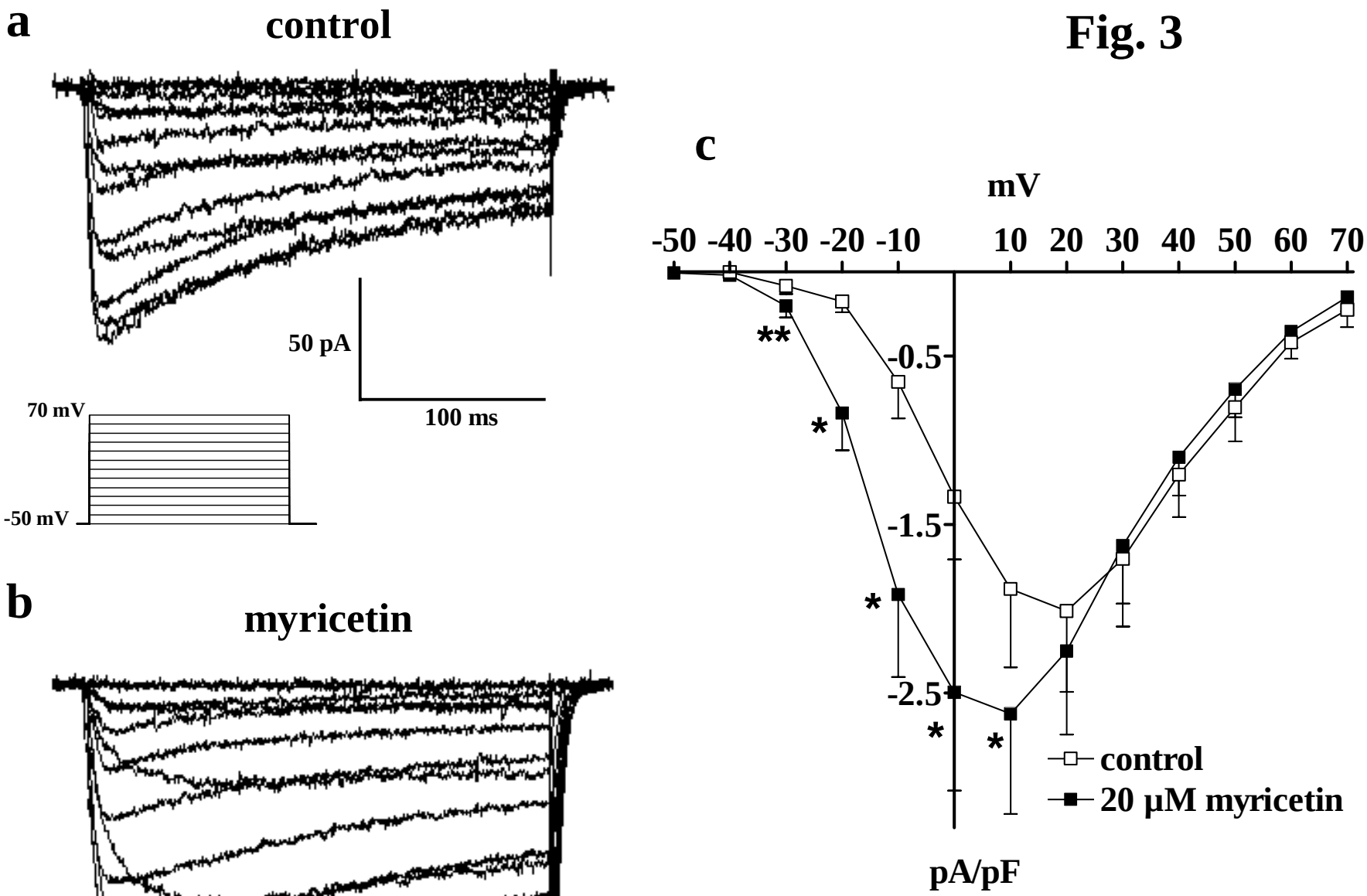

JPET Fast Forward. Published on January 21, 2005 as DOI: 10.1124/jpet.104.080135
This article has not been copyedited and formatted. The final version may differ from this version.

Fig. 4

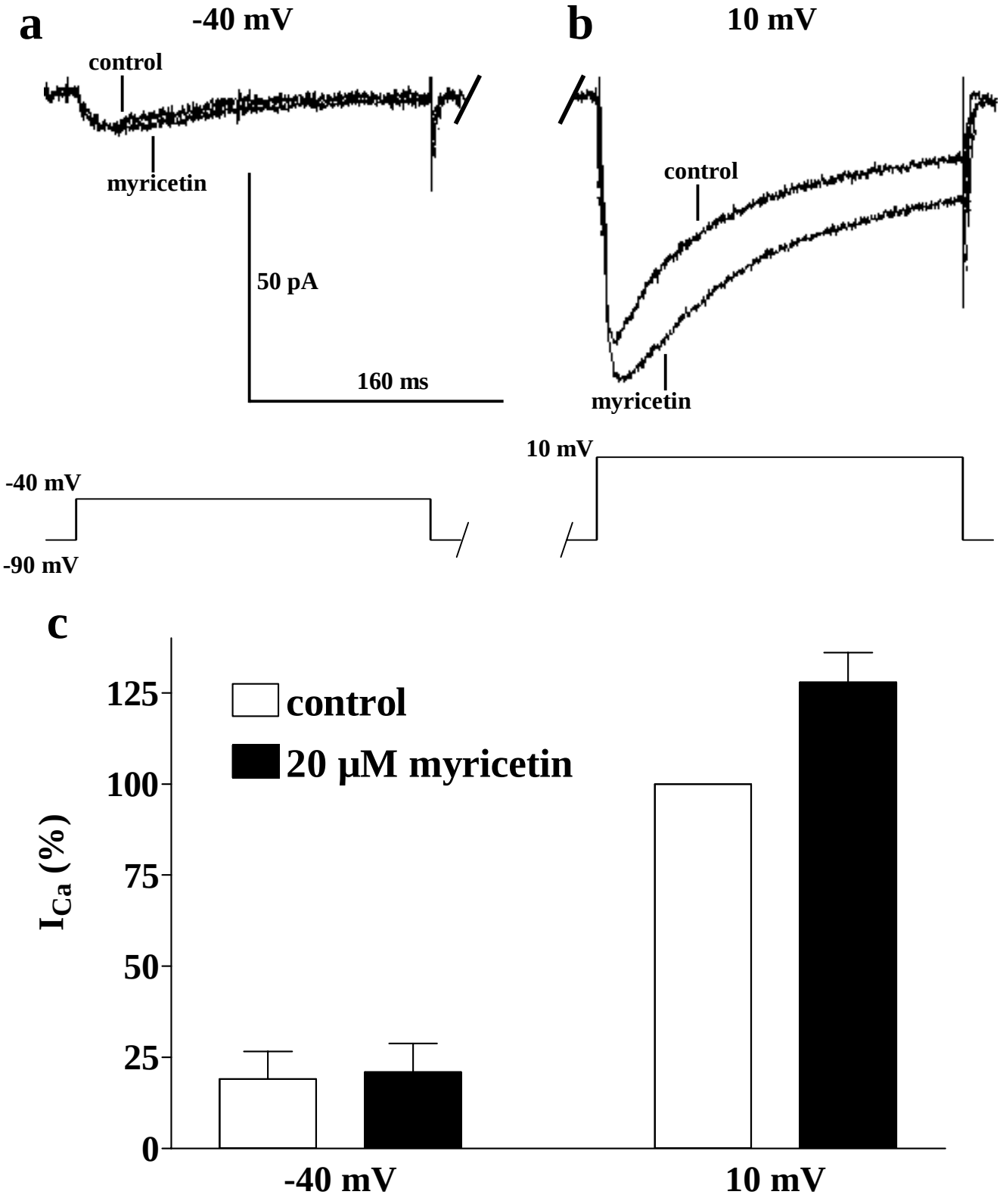

JPET Fast Forward. Published on January 21, 2005 as DOI: 10.1124/jpet.104.080135
This article has not been copyedited and formatted. The final version may differ from this version.

Fig. 5

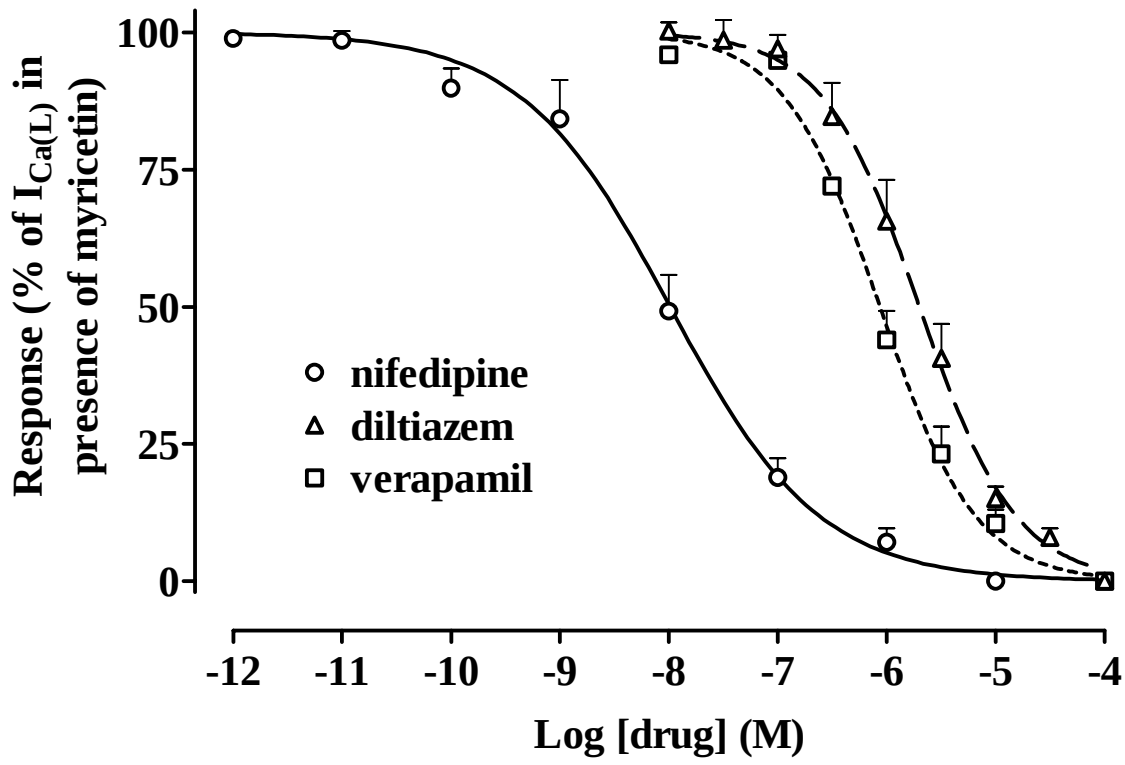

JPET Fast Forward. Published on January 21, 2005 as DOI: 10.1124/jpet.104.080135
This article has not been copyedited and formatted. The final version may differ from this version.

Fig. 6

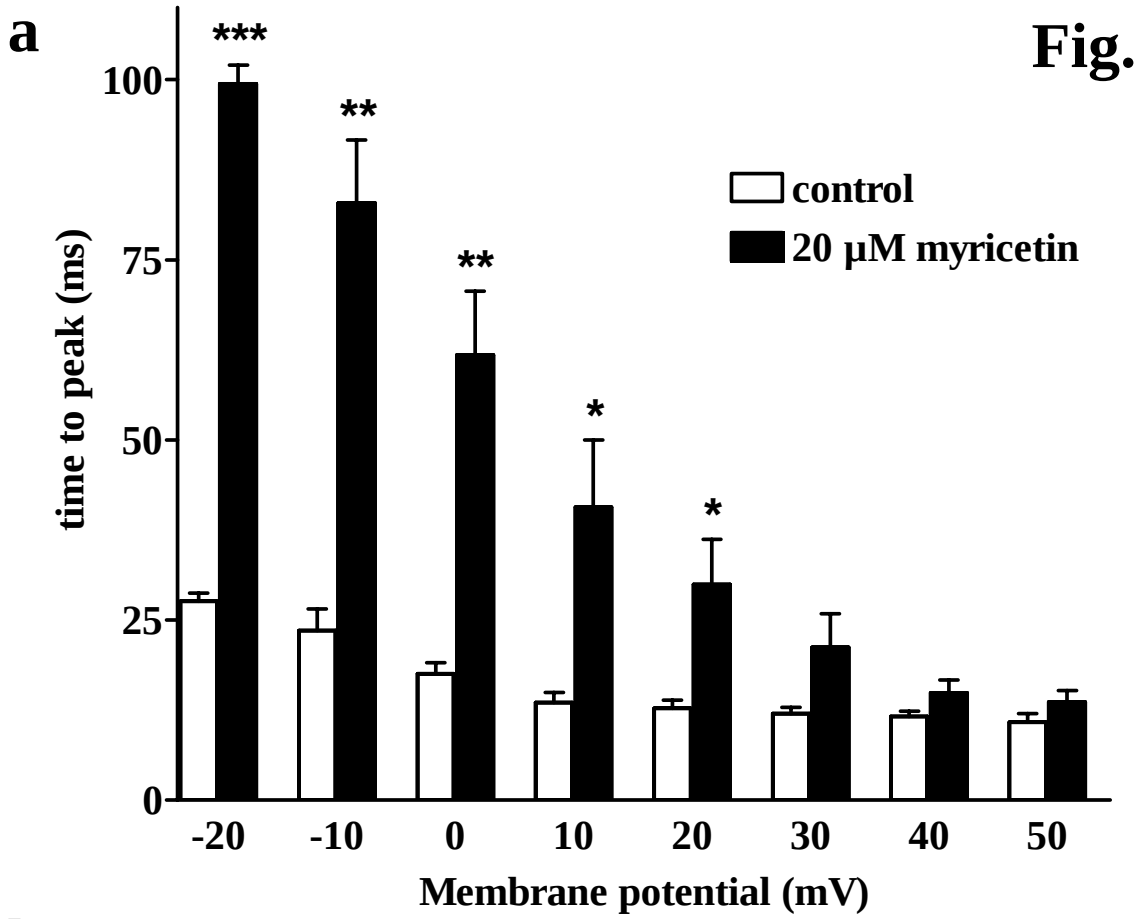

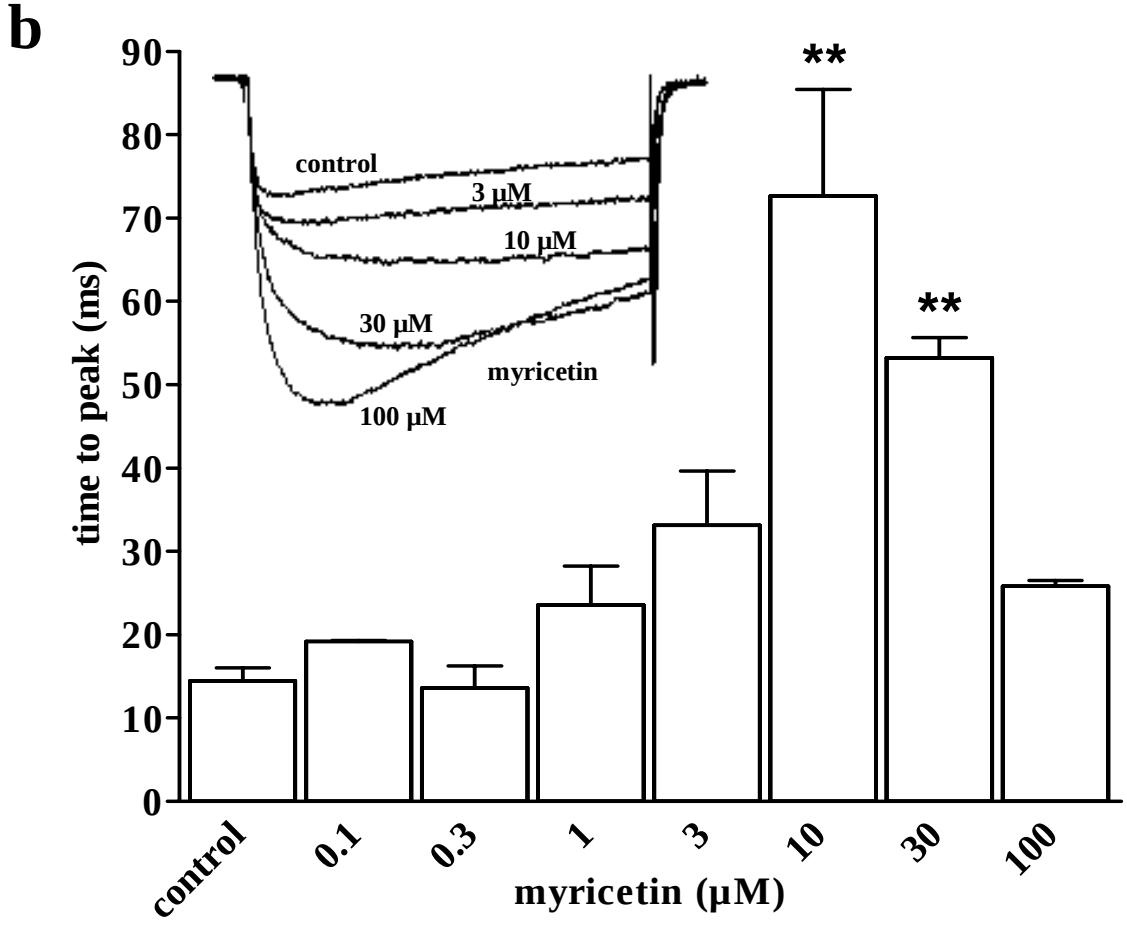

JPET Fast Forward. Published on January 21, 2005 as DOI: 10.1124/jpet.104.080135
This article has not been copyedited and formatted. The final version may differ from this version.

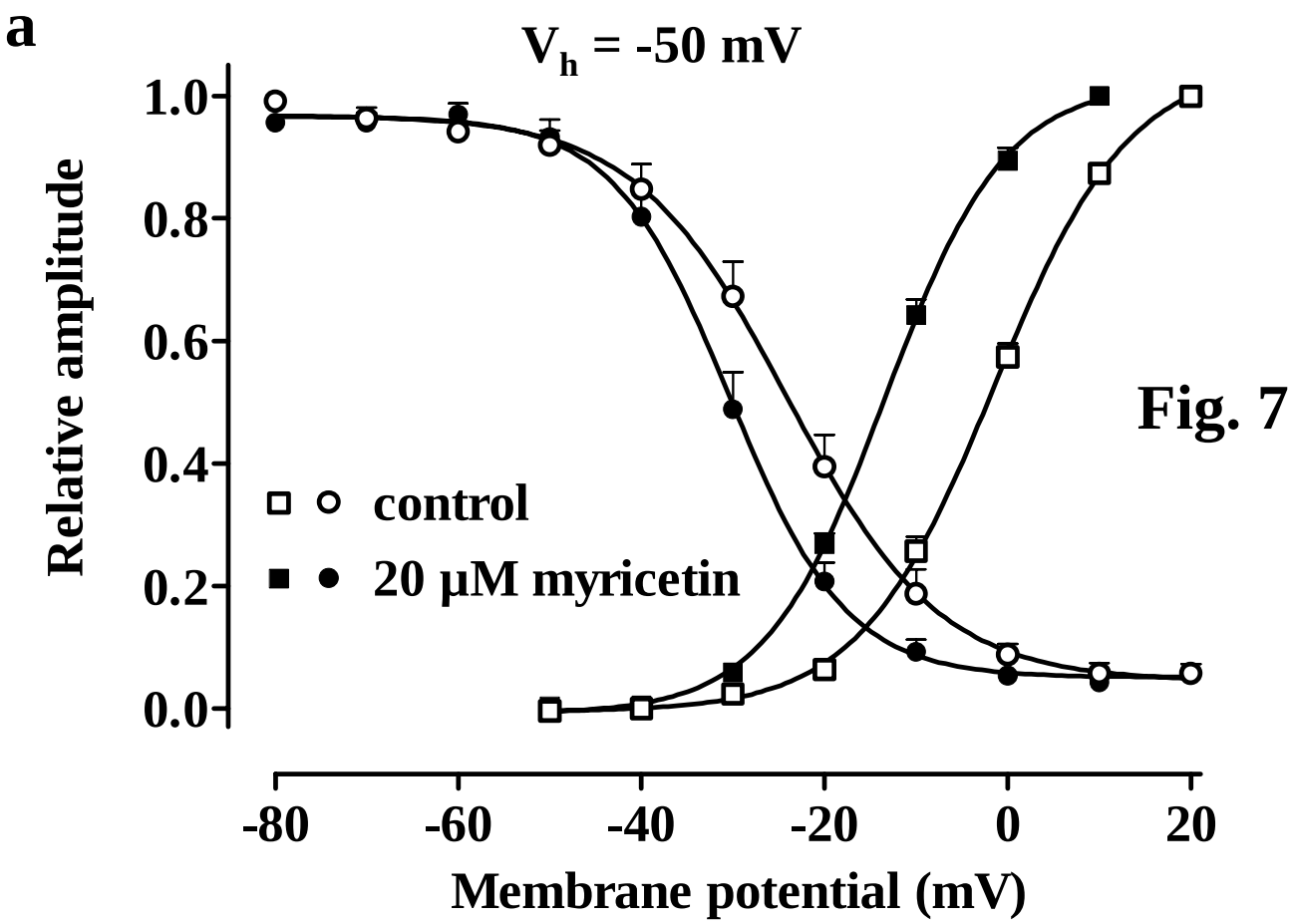

Fig. 7

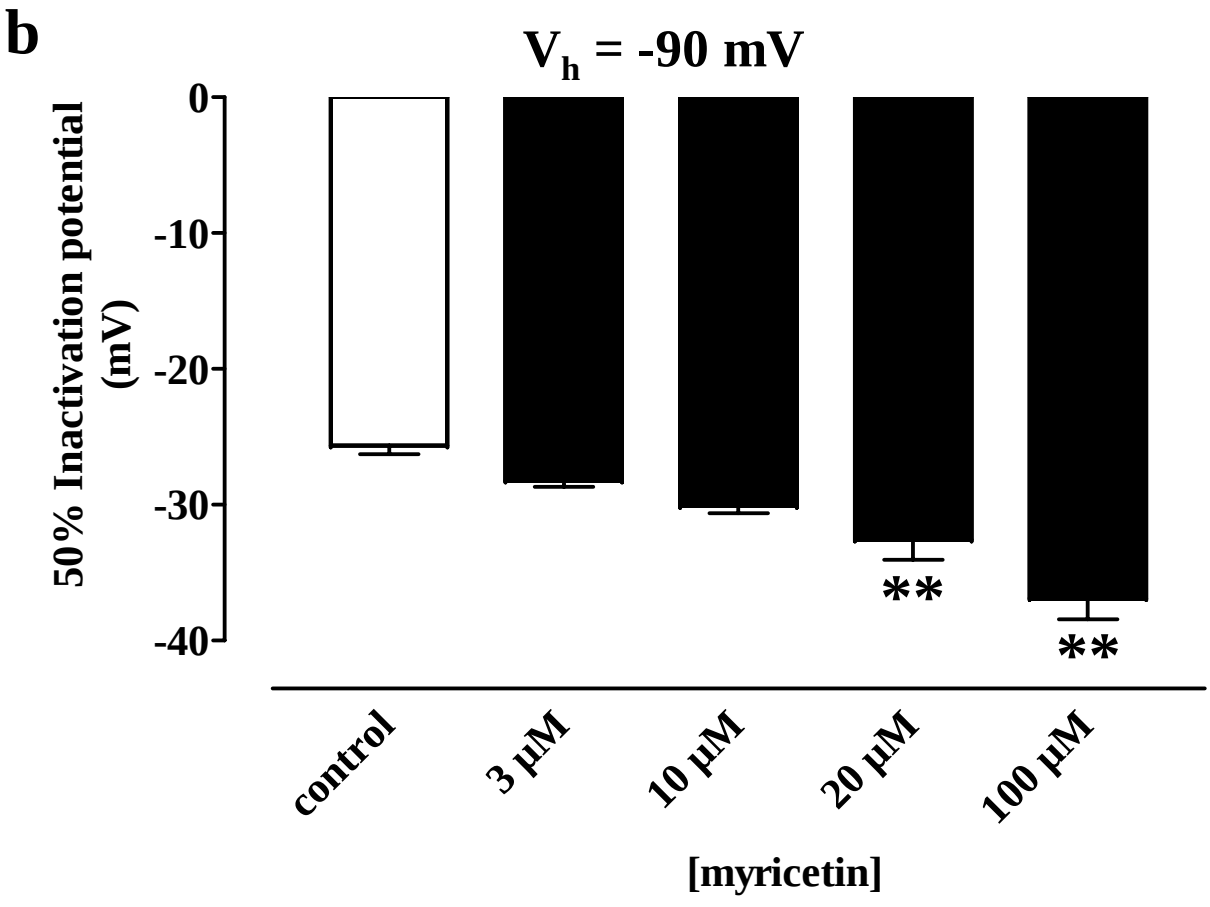

JPET Fast Forward. Published on January 21, 2005 as DOI: 10.1124/jpet.104.080135
This article has not been copyedited and formatted. The final version may differ from this version.

Fig. 8